Revelation of Multiple Underlying RuO_2 Redox Processes Associated with Pseudocapacitance and Electrocatalysis

Chong-Yong Lee and Alan M. Bond*

School of Chemistry, Monash University, Clayton, Victoria 3800, Australia

*Corresponding author. E-mail: alan.bond@sci.monash.edu.au. Tel: +61 3 9905 1338. Fax: +61 3 9905 4597.

Supporting Information

Table S1 Experimental values of $I^p_{4\omega t}$, $I^p_{5\omega t}$ and $I^p_{6\omega t}$ and their corresponding peak potentials for the redox centres A′, Ru(III/II); B′, Ru(IV/III); C′, Ru(IV/V) and D′, Ru(V/VI) as a function of H_2SO_4 concentration (0.5 M to 3.0 M) derived from anhydrous RuO_2 and hydrated $RuO_2.nH_2O$ (500 ^oC) thin film modified glassy carbon electrodes. The values of the ratio provided in Table 1 $I^p_{4\omega t}/I^p_{6\omega t} : I^p_{5\omega t}/I^p_{6\omega t}$ are calculated from data in this table, where $I^p_{4\omega t}$, $I^p_{5\omega t}$ and $I^p_{6\omega t}$ represent the peak current magnitudes of the fourth, fifth and sixth ac harmonics, respectively.

Sample	H_2SO_4 Conc. (M)		Redox centre A′ [Ru(III/II)]	Redox centre B′ Ru(IV/III)]	Redox centre C′ [Ru(IV/V)]	Redox centre D′ [Ru(V/VI)]
RuO_2	0.50	$I^p_{n\omega t}$ (μA)[a]	3.48,0.80,0.18	4.60,2.5,1.27	5.15,1.60,0.59	6.40,2.43,1.38
		$E^p_{n\omega t}$ (V)[b]	0.32,0.32,0.32	0.52,0.52,0.52	1.00,1.00,1.00	1.13,1.12,1.13
		ratio[c]	19:4.4	3.6:2.0	8.7:2.7	4.6:1.8
	1.00	$I^p_{n\omega t}$ (μA)[a]	3.76,1.00,0.17	4.64,2.77,1.27	7.50,2.31,0.93	6.97,3.30,2.18
		$E^p_{n\omega t}$ (V)[b]	0.35,0.35,0.34	0.54,0.53,0.53	1.03,1.03,1.03	1.16,1.15,1.16
		ratio[c]	22:5.9	3.7:2.2	8.1:2.5	3.2:1.5
	2.00	$I^p_{n\omega t}$ (μA)[a]	4.12,1.11,0.25	4.94,2.95,1.47	9.23,3.06,1.05	7.12,3.45,2.20
		$E^p_{n\omega t}$ (V)[b]	0.37,0.38,0.38	0.55,0.55,0.55	1.06,1.06,1.06	1.19,1.19,1.19
		ratio[c]	17:4.4	3.4:2.0	8.8:2.9	3.2:1.6
	3.00	$I^p_{n\omega t}$ (μA)[a]	4.58,1.23,0.24	4.80,2.99,1.42	10.2,3.36,1.06	8.00,4.35,2.71
		$E^p_{n\omega t}$ (V)[b]	0.39,0.40,0.41	0.57,0.56,0.56	1.09,1.09,1.09	1.21,1.22,1.23
		ratio[c]	19:5.1	3.4:2.1	9.6:3.2	3.0:1.6
$RuO_2.nH_2O$ (500^oC)	0.50	$I^p_{n\omega t}$ (μA)[a]	13.2,3.88,1.16	9.27,4.89,2.12	13.3,5.05,2.17	39.1,17.8,7.01
		$E^p_{n\omega t}$ (V)[b]	0.29,0.29,0.29	0.54,0.54,0.55	0.96,0.96,0.96	1.17,1.16,1.16
		ratio[c]	11:3.4	4.4:2.3	6.1:2.3	5.6:2.5
	1.00	$I^p_{n\omega t}$ (μA)[a]	15.1,4.43,1.45	7.62,2.86,1.45	26.5,8.15,3.52	60.0,23.2,10.2
		$E^p_{n\omega t}$ (V)[b]	0.31,0.31,0.32	0.55,0.55,0.55	1.01,1.00,1.01	1.21,1.19,1.19
		ratio[c]	10:3.1	5.3:2.0	7.5:2.3	5.9:2.3
	2.00	$I^p_{n\omega t}$ (μA)[a]	16.8, 4.32, 1.61	7.41;3.46,1.56	29.2,10.5,3.89	69.6, 30.5,13.0
		$E^p_{n\omega t}$ (V)[b]	0.34,0.35,0.35	0.56,0.56,0.56	1.05,1.05,1.05	1.23,1.23,1.24
		ratio[c]	10:2.7	4.8:2.2	7.5:2.7	5.4:2.4
	3.00	$I^p_{n\omega t}$ (μA)[a]	15.5,4.54,1.85	7.44,3.50,1.55	30.8,11.6,3.70	74.5,27.5,12.5
		$E^p_{n\omega t}$ (V)[b]	0.37,0.37,0.36	0.58,0.57,0.57	1.08,1.08,1.08	1.26,1.25,1.25
		ratio[c]	8.4:2.5	4.8:2.3	8.3:3.1	6.0:2.2

[a] $I^p_{n\omega t}$ (n = 4,5,6). [b] $E^p_{n\omega t}$ (n = 4,5,6) is the peak potential corresponding to $I^p_{n\omega t}$. [c]ratio of $I^p_{4\omega t}$ and $I^p_{5\omega t}$ to $I^p_{6\omega t}$.

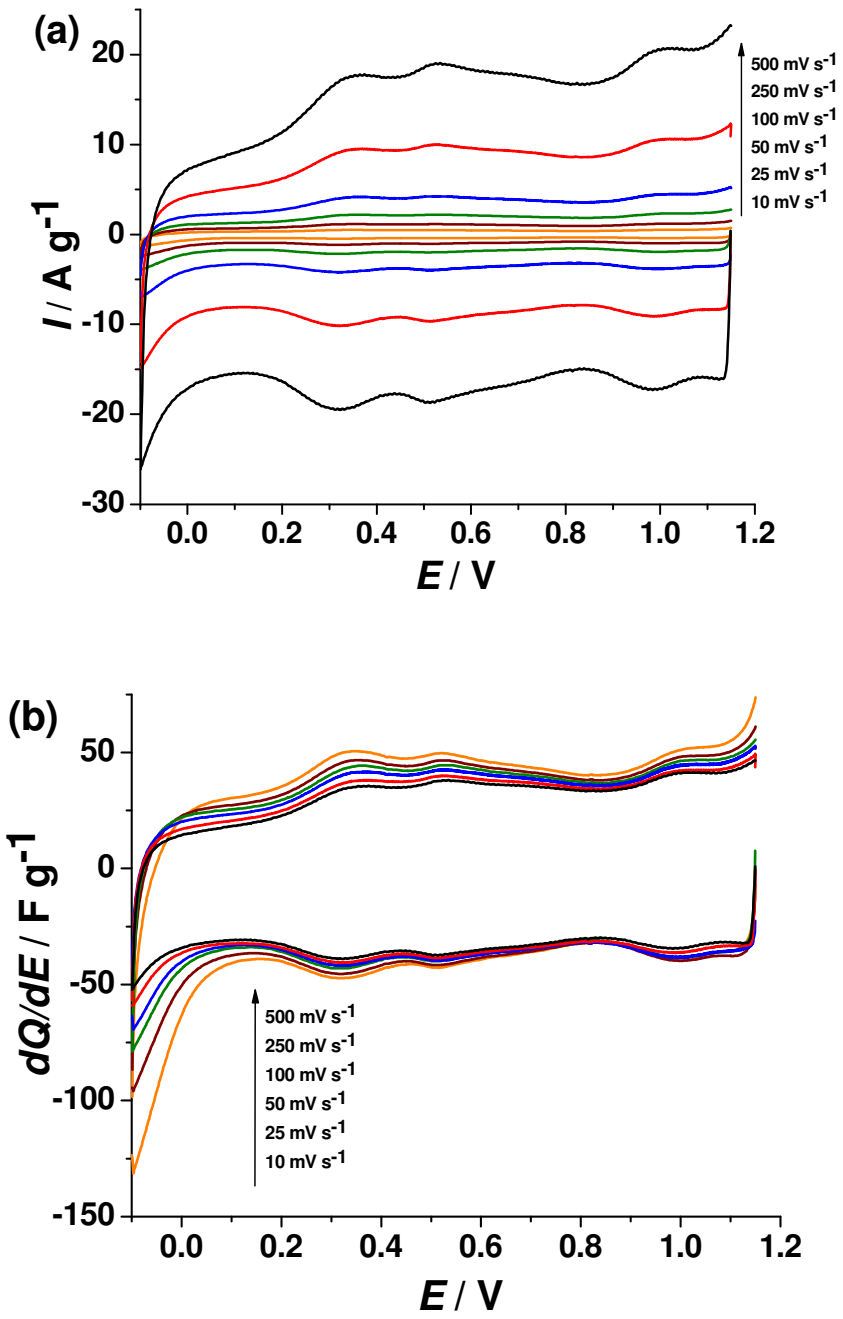

Figure S1 (a) Dc cyclic voltammograms obtained from an anhydrous RuO_2 thin film modified glassy carbon electrode in contact with 0.5 M H_2SO_4 aqueous electrolyte solution at designated scan rates. (b) Differential capacitance derived from dc cyclic voltammograms provided in (a).

Figure S1 illustrates the behavior of thin film electrode in the format presented by Sugimoto et. al.,[S1, S2] who derived the electric double layer capacitance (C_{dl}), adsorption related charge (C_{ad}), and the irreversible redox related charge (C_{irr}) from dc voltammograms presented in the differential capacitance per unit mass of electrode material.

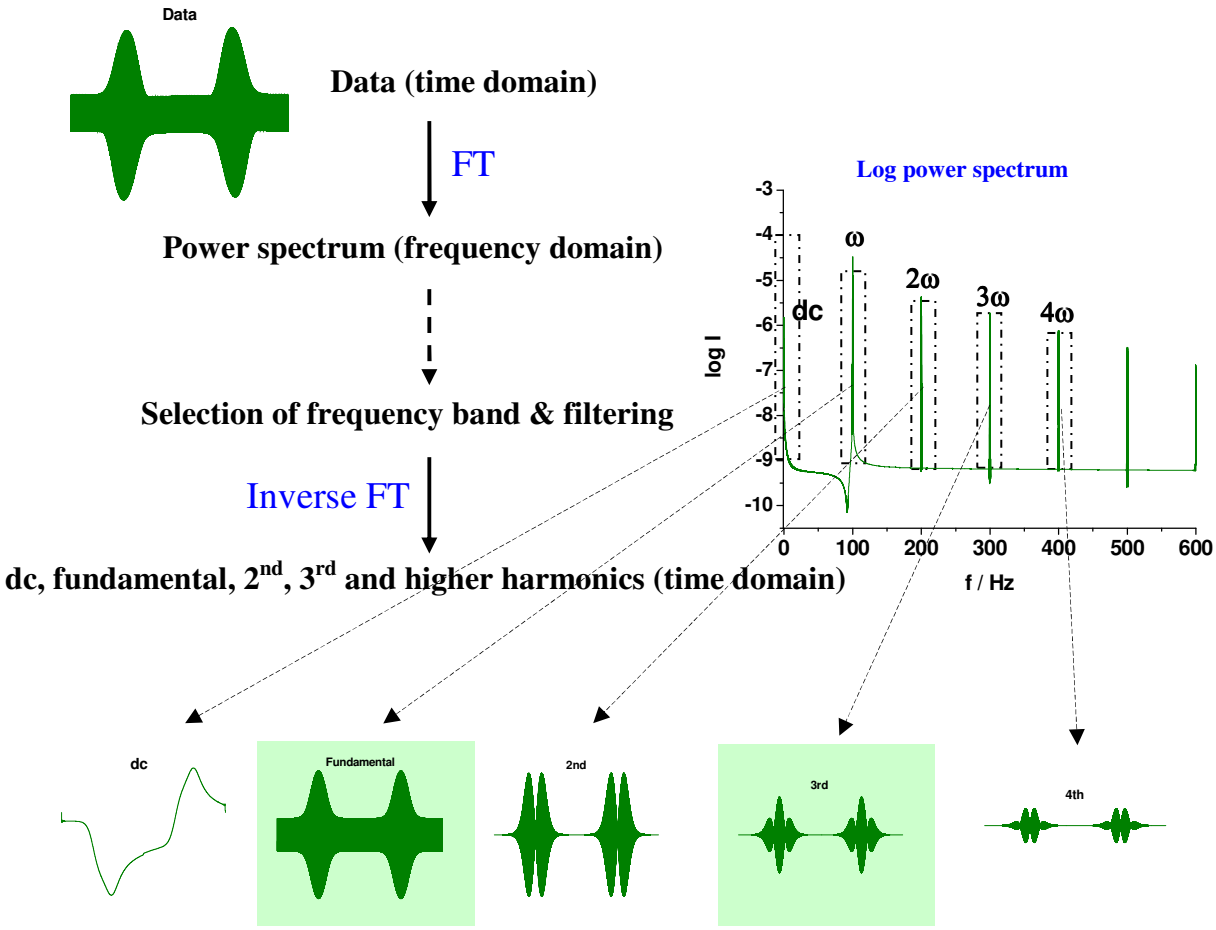

Figure S2 Schematic illustration of the data processing sequences used in large-amplitude FT ac voltammetry.

Figure S2 provides details of the data processing strategy used in large-amplitude FT ac voltammetry.[S3] Initially, the total (dc and ac) current are collected as a function of the time. The FT algorithm is then used to convert the time domain data to the frequency domain and present the output in the form of a power spectrum. In order to obtain the individual harmonic components, the relevant region (dc or harmonic of interest) in the power spectrum is selected and the power of all other frequencies is set to zero. Application of the inverse Fourier transform then gives the required component. The current component that corresponds to the applied frequency, ω is designated as the fundamental harmonic, while the second, third, fourth, fifth etc. harmonic current components are associated with the response at frequencies of 2ω, 3ω, 4ω, 5ω, respectively. There is also an aperiodic dc component that resembles a conventional cyclic voltammogram, but differs slightly because of the presence of sinusoidal modulation.

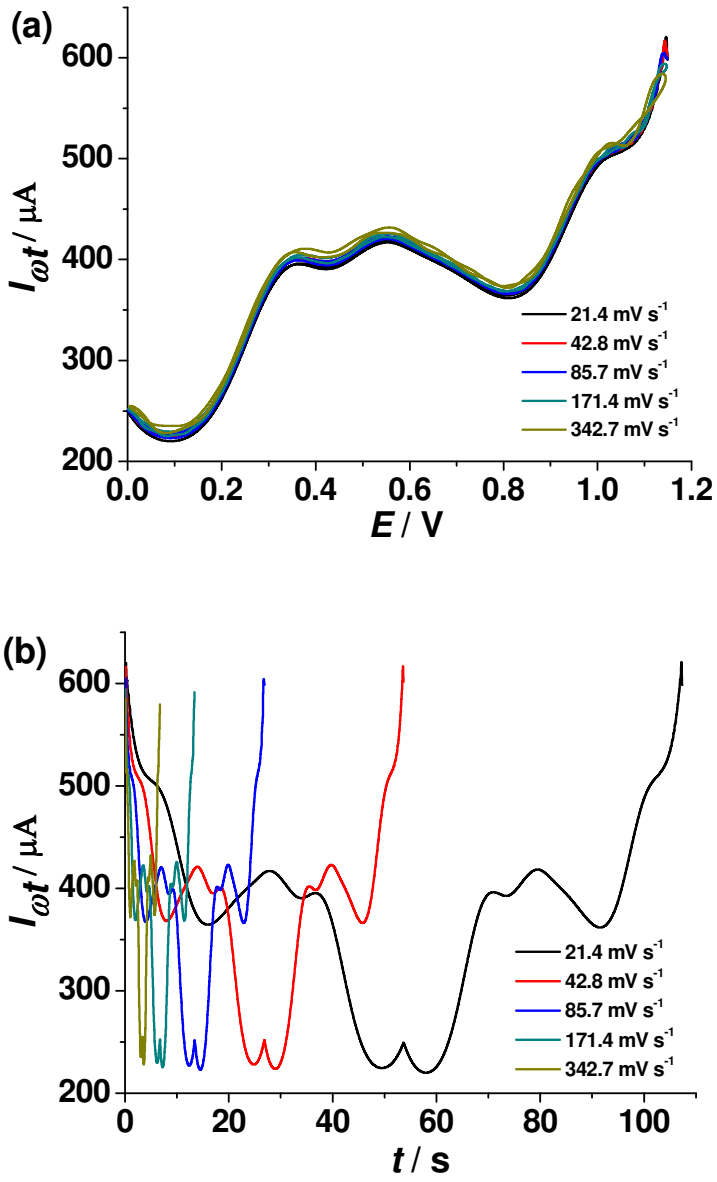

Figure S3 Dependence of FT-ac fundamental harmonic component on scan rate when an anhydrous RuO_2 thin film modified glassy carbon electrode is in contact with 0.5 M H_2SO_4 aqueous electrolyte. (a) voltage-axis and (b) time-axis format. Experimental conditions: E_{start} = 1.36 V, E_{switch} = 0.20 V, f = 9.0 Hz and ΔE = 0.08 V.

Figure S3a shows the fundamental ac harmonic component is essentially independent of scan rate even though this parameter influences the time scale (Fig. S3b). Equivalently, the second and higher order harmonic components are also independent of scan rate. In comparison, in dc voltammetry (Fig. S1a), the scan rate contributes significantly to the value of the peak current magnitude.

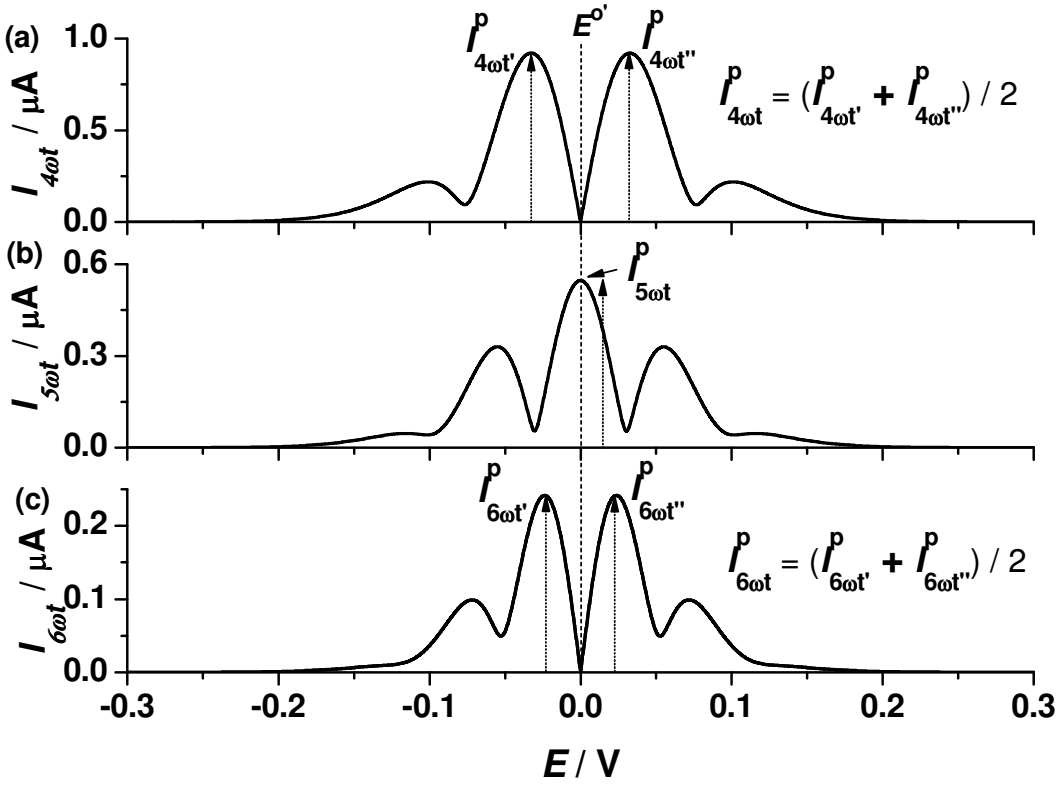

Figure S4 Illustration of the methods used to determine analogues of dc voltammetric mid-point potentials (E_m) and ac harmonic peak current magnitudes for (a) fourth, (b) fifth and sixth ac harmonics.

Figure S4 illustrates the procedures used to analyze the higher harmonic ac data. The first step is to estimate the E_m of the redox centre. This can be estimated as shown from the average of the dc peak potentials (see Fig. 1). For the odd (fifth) harmonic peak current value, $I^p_{5\omega t}$ is derived from the central lobe that exhibits the maximum peak current magnitude. In the case of the even (fourth and sixth) harmonics, the peak currents, $I^p_{4\omega t}$ and $I^p_{6\omega t}$ represent the average values of the two lobes having the maximum current. Note that this example is based on simulation of a simple process that exhibits fast electron transfer. In the case of slow electron transfer or rate determining coupled protonation steps, symmetry may be lost. In this case, reference to the E_m is used via the strategy shown in Fig. 1.

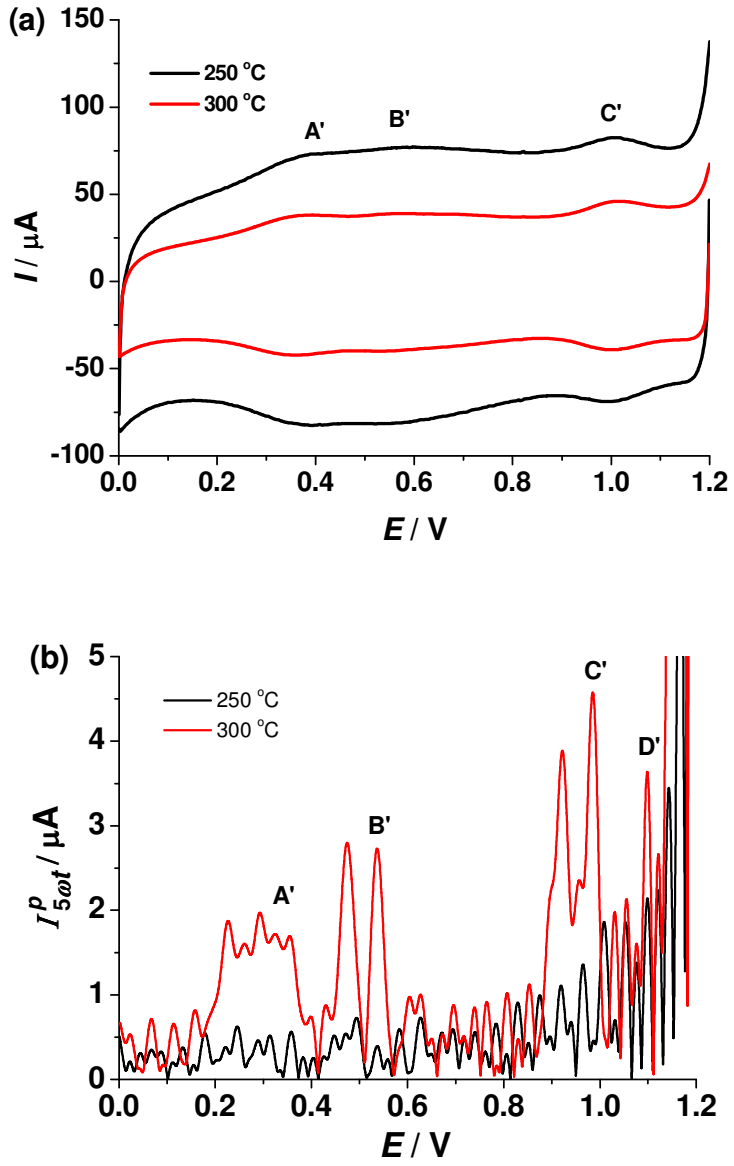

Figure S5 (a) Dc (v = 0.045 V s^{-1}) and (b) fifth harmonic FT-ac cyclic voltammograms obtained when a $RuO_2.nH_2O$ (heat-treated at 250 °C or 300 °C) thin film modified glassy carbon electrode is in contact with 0.5 M H_2SO_4 aqueous electrolyte. For the FT-ac experiments: E_{start} = 1.20 V, E_{switch} = 0.00 V, f = 9.0 Hz, ΔE = 0.08 V and v = 0.045 V s^{-1}.

The decrease in water content of the hydrated $RuO_2.nH_2O$ that occurs upon heat-treatment gives rise to a decrease in the double layer capacitance (Fig. S6a). The background current detected after heat-treatment at 300 °C is nearly half that found with heat-treatment at 250 °C. In the ac fifth harmonic component (Fig. S6b), the faradaic processes associated with the hydrated $RuO_2.nH_2O$ sample heat-treated at 250 °C are weak. In contrast, all four ruthenium based processes at ac fifth harmonic become well defined after heat-treatment at ≥ 300 °C.

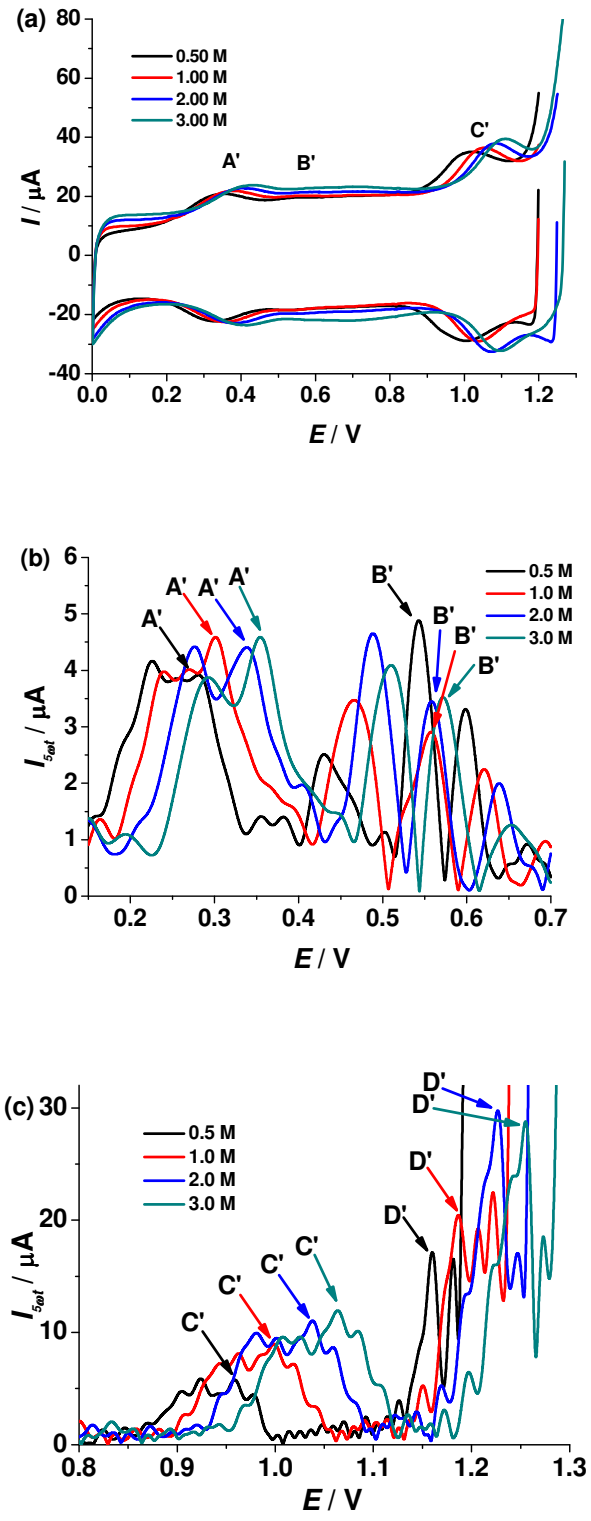

Figure S6 (a) Dc (v = 0.045 V s^{-1}) and (b)-(c) Fifth harmonic FT ac cyclic voltammograms obtained from an hydrated RuO2.nH2O (500 ^{o}C) thin film modified glassy carbon electrode in contact with designated H_2SO_4 concentrations (0.5 M to 3.0 M). For the FT ac voltammetric experiments: f = 9.0 Hz, ΔE = 0.08 V, E_{switch} = 0.00 V and in 0.5 M H_2SO_4 (E_{start} = 1.20 V, v = 0.045 Vs^{-1}); 1.0 M H_2SO_4 (E_{start} = 1.25 V, v = 0.047 Vs^{-1}); 2.0 M H_2SO_4 (E_{start} = 1.27 V, v = 0.047 Vs^{-1}) and 3.0 M H_2SO_4 (E_{start} = 1.30 V, v = 0.048 Vs^{-1}). Processes A′, B′, C′ and D′ are assigned to Ru(III)/(II), Ru(IV)/(III), Ru(IV)/(V) and Ru(V)/(VI), respectively.

References

[S1] Sugimoto, W., Kizaki, T., Yokoshima, K., Murakami, Y., Takasu, Y. Evaluation of the pseudocapacitance in RuO_2 with a RuO_2/GC thin film electrode Electrochim. Acta. **49**, 313-320 (2004).

[S2] Sugimoto, W.; Yokoshima, K.; Murakami, Y.; Takasu, Y. Charge storage mechanism of nanostructured anhydrous and hydrous ruthenium-based oxides. Electrochim. Acta. **52**, 1742-1748 (2006).

[S3] Bond, A. M., Duffy, N. W., Guo, S.-X., Zhang J. & Elton, D. M. Changing the look of voltammetry: can FT revolutionize voltammetric techniques as it did for NMR? *Anal. Chem.* **77**, 186A-195A (2005).